Solving Einstein Field Equations on a quantum computer

Clelia Altomonte (she/her)
(clelia.altomonte@kcl.ac.uk)
PhD supervisor: Prof. Malcolm Fairbairn

King's College London,
Physics Department,
Theoretical Particle Physics and Cosmology Group

KEK, Tsukuba
Concepts of Quantum and Spacetime Workshop
12 March 2026

Abstract

Computationally expensive simulations performed on classical computers such as those of numerical general relativity (NR) can be tackled by quantum algorithms for solving systems of pdes, with the possibility to obtain a quantum advantage in terms of computational resources and speed up in runtime with respect to classical counterparts.

Outline

I. Introduction and motivation

II. Mathematical details
Mappings: WEBB $\rightarrow$ Dirac Hamiltonian $\rightarrow$ LB $\rightarrow$ QW

III. Constructing the algorithm
Amplitude encoding
Advection
Collision
Lapse and Shift subroutines

IV. Testing the algorithm
Schwarzschild BH stationary solution
Quasinormal modes

V. Conclusion and future work

Introduction and motivation

Quantum computing for Physics problems

"Nature isn't classical, dammit, and if you want to make a simulation of nature, you'd better make it quantum mechanical, and by golly it's a wonderful problem, because it doesn't look so easy" [Feynman, 1982].

The current **Quantum Utility Era** [Kim et al., 2023], with the availability of Noisy Intermediate Scale Quantum (NISQ) computers, makes it possible to:

- perform such **quantum mechanical simulations of Nature** by means of Hamiltonian simulation on digital and analogue quantum computing platforms;
- solve **classical problems** in a more efficient way through **quantum algorithms** that, leveraging quantum mechanical properties such as entanglement and superposition, achieve a **quantum advantage**[1] with respect to classical counterparts.

[1] quantifiable through the computational complexity framework in terms of runtime as a function of input size.

Quantum computing overview: advantages

Quantum computing

computational model that follows the rules of quantum mechanical statistics.

Advantages

- QM resources: superposition, interference, entanglement.
- move problems between computational complexity classes (quantum advantage).

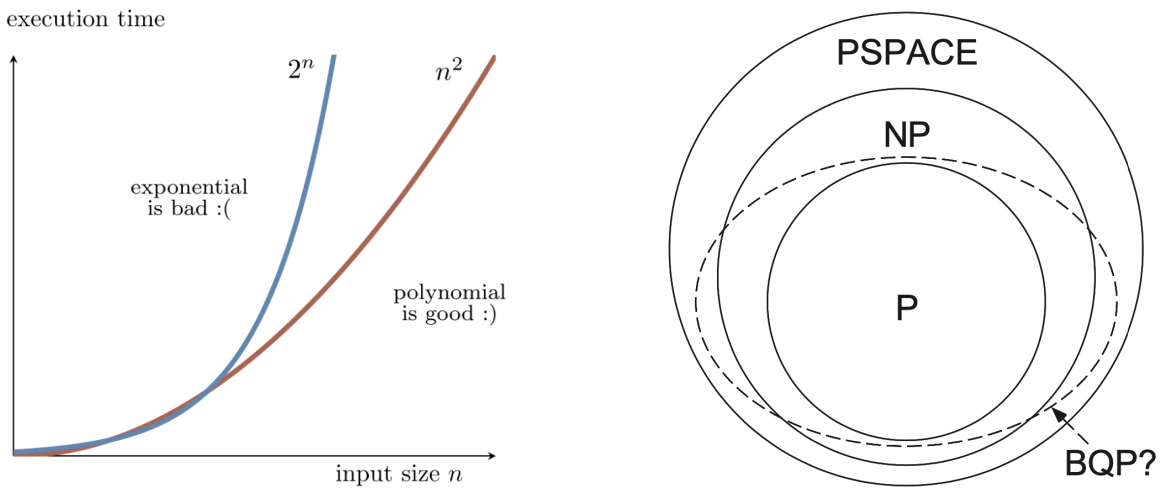

Figure: left: exponential vs polynomial execution time [n.d.(b)]; right: computational complexity classes [Nielsen and Chuang, 2012]

Quantum computing overview: disadvantages and solutions

Drawbacks

- decoherence-induced errors (Noisy Intermediate-Scale Quantum devices, NISQ) and measurement-induced collapse of ψ (cf. quantum tomography).
- unitary evolution.

Solutions

- error-correcting codes, weak measurements protocols.
- Stinespring dilation, open-system evolution, entanglement, effective potential methods from quantum chemistry/condensed matter, etc.

Numerical General Relativity

- Numerical General Relativity (nGR) is the research field that studies numerical methods and algorithms to solve the Einstein Field Equations (EFE)

$$G_{\mu\nu} + \Lambda g_{\mu\nu} = \kappa T_{\mu\nu}$$

- The ADM formalism [1] for nGR is based on a 3+1 foliation of spacetime, and on the time evolution of the 3-metric defined on each foliated hypersurface through a Hamiltonian.

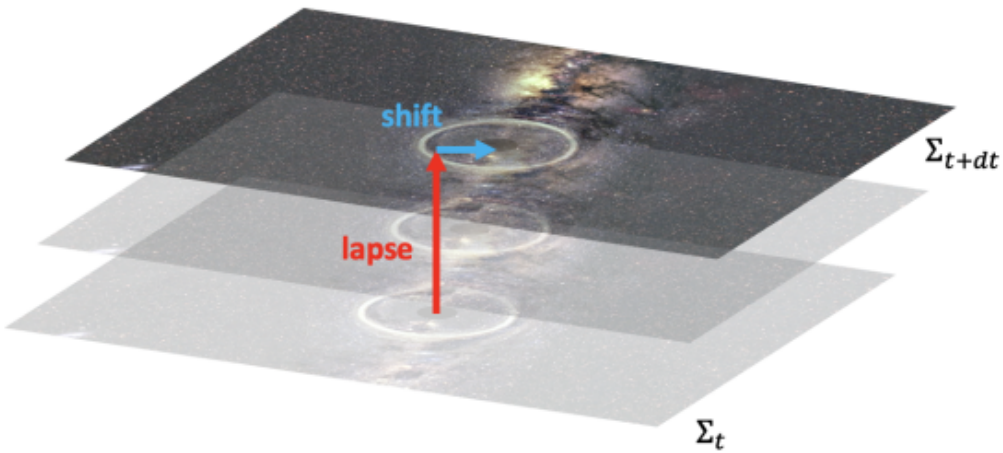

Fig. 1: Scheme of ADM spacetime foliation with lapse and shift functions (using a black hole visualization by NASA/JPL-Caltech/R. Hurt (IPAC))

Applying quantum computing to numerical relativity: our strategy

• The WEBB hyperbolic tetrad formalism differs from ADM in evolving connection coefficients (Ricci rotation coefficients) rather than the metric, and is particularly suitable for a quantum computing implementation due to:

- Ricci rotation coefficients are scalar fields $\rightarrow$ vector amplitude encoding;
- first-order symmetrizable evolution pde's $\rightarrow$ Hamiltonian simulation:
- Hamiltonian mapping $\rightarrow$ similarities to quantum algorithms with known quantum advantage and resource-efficient way to treat nonlinearities through operator splitting;

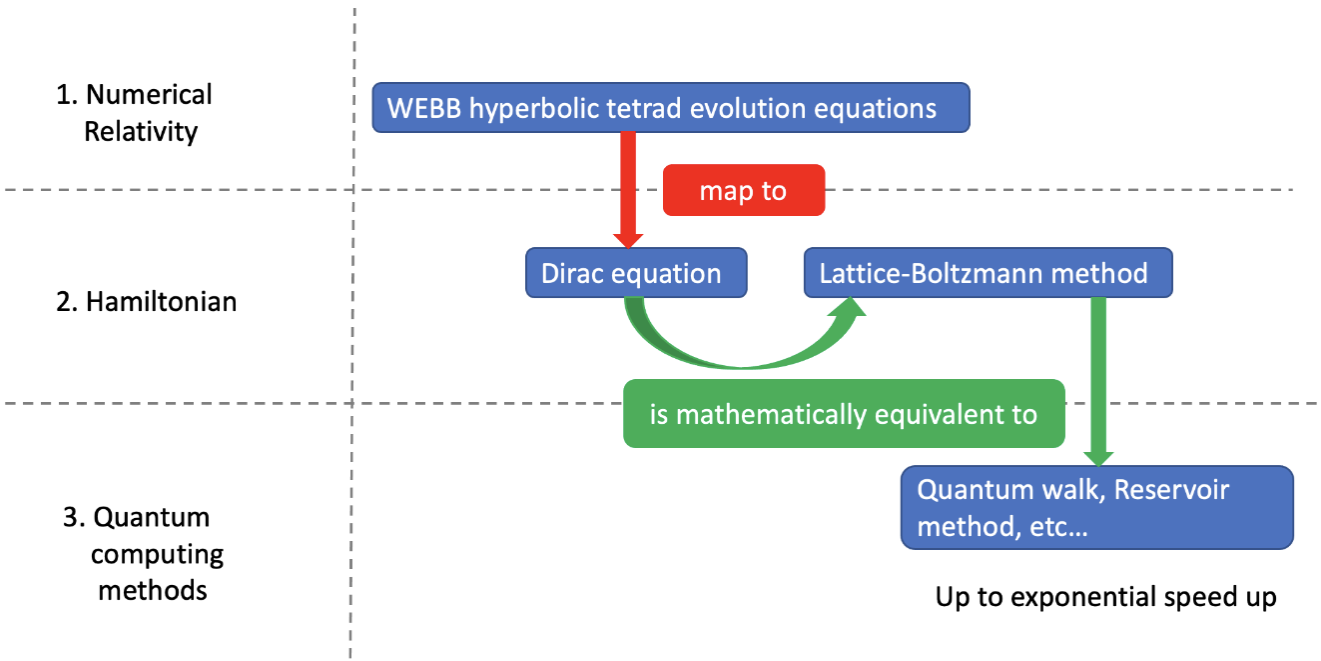

Mathematical details

Mappings: WEBB $\rightarrow$ Dirac Hamiltonian $\rightarrow$ LB $\rightarrow$ QW

1. Numerical Relativity: WEBB hyperbolic tetrad formalism

$$D_0\mathbf{q} + M^a D_a \mathbf{q} = \mathbf{S} \tag{1}$$

2. Mapping to Dirac Hamiltonian[2] ($\rightarrow$ LB $\rightarrow$ QW)[3]

$$\boldsymbol{q} \rightarrow \psi(t, \mathbf{x}) \rightarrow \text{Amplitude encoding} \tag{2}$$

$$M^a D_a \rightarrow \boldsymbol{\alpha} \cdot \hat{\mathbf{p}} \rightarrow \text{Advection} \tag{3}$$

$$\boldsymbol{S} \rightarrow e I_4 V(\mathbf{x}, t) \rightarrow \text{Collision} \tag{4}$$

3. Operator splitting[4]

$$\psi\left(t_{n+1}\right) = \prod_{k=1}^{N_{\text{seq}}} \left[e^{-i s_0^{(k)} \Delta t \mathcal{T}} \prod_{j=1}^{N_{\text{op}}} e^{-i s_j^{(k)} \Delta t \widehat{H}_j(t_n)} \right] \psi\left(t_n\right) + O\left(\Delta t^q\right) \tag{5}$$

[2] [Fillion-Gourdeau, MacLean, and Laflamme, 2017]
[3] Succi, Fillion-Gourdeau, and Palpacelli, 2015
[4] [Fillion-Gourdeau, MacLean, and Laflamme, 2017]

Constructing the algorithm

Amplitude encoding

- Amplitude encoding $\rightarrow$ encode the 2^n grid-points discretisation of 2^m fields using $n + m$ qubits.
- Quantum superposition $\rightarrow$ parallelization of operations.
- lattice-Boltzmann method $\rightarrow$ global operations only act on *spin* register's m qubits.

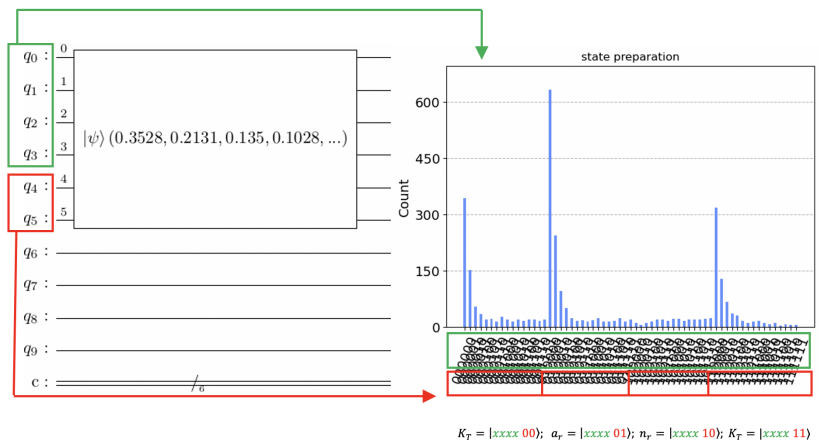

Figure: Amplitude encoding

$$D_0\mathbf{q} + \mathcal{C}^{\hat{r}} B_R \partial_r \mathbf{q} = \mathbf{S}.$$

$$D_0 = \frac{1}{\alpha}(\partial_t - \beta^r \partial_r)$$

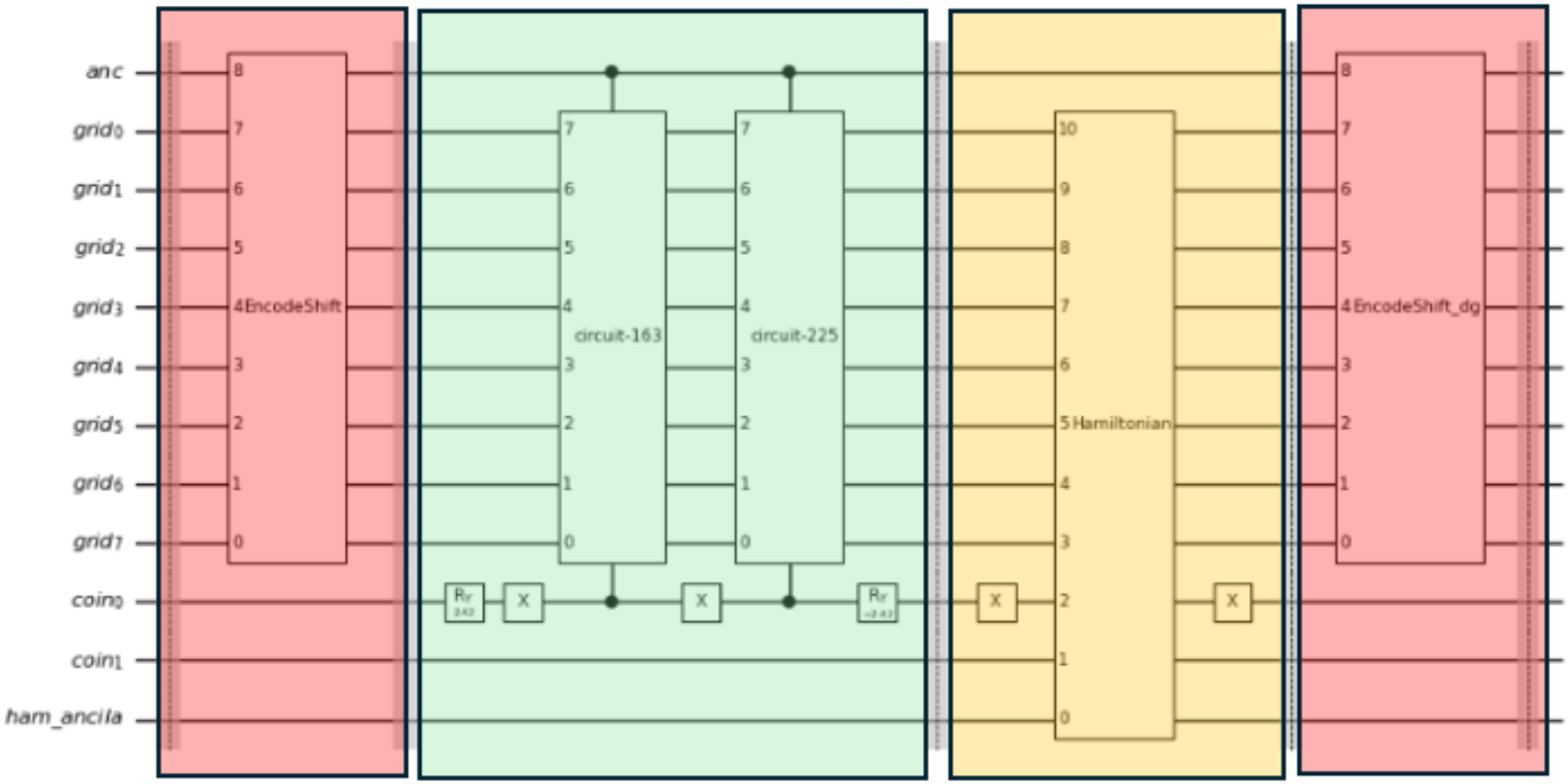

Advection

1. Rotate q to eigenvectors basis where C^r is $\mathrm{diag}(1, -1, 1, -1)$;
2. Perform advection through increase/decrease controlled gates;
3. Rotate q back;

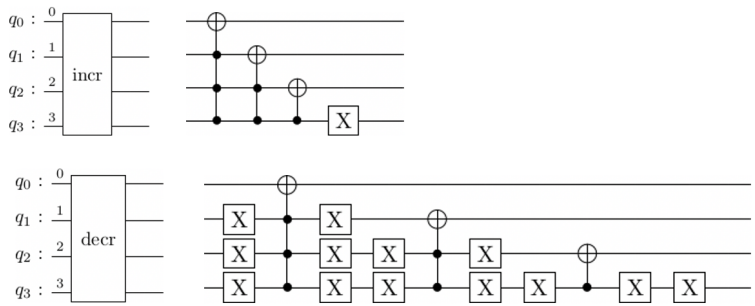

Figure: left: Advection step; right: increase/decrease gates

Collision

$$S = f\left(\begin{bmatrix} K_R \\ a_r \\ K_T \\ n_r \end{bmatrix}\right) = \begin{bmatrix} f_1(K_R, a_r, K_T, nr) \\ f_2(K_R, a_r, K_T, nr) \\ f_3(K_R, a_r, K_T, nr) \\ f_4(K_R, a_r, K_T, nr) \end{bmatrix} = \begin{bmatrix} a_r^2 - n_r^2 - K_R^2 + K_T^2 + \frac{2n_r}{R} \\ \frac{a_r + n_r}{R} + K_R K_T - K_T^2 - n_r^2 - a_{\hat{\mu}} n_r \\ \frac{K_T - K_R}{R} - a_r K_T + n_r (K_R - 2K_T) \\ \frac{2(K_R - K_T)}{R} \end{bmatrix} \quad (6)$$

There are different possible approaches to model non-linear terms in S. We used:

1. total derivatives encoded in Jacobian matrix
2. build transition/scattering matrix
3. Stinespring dilation (Hermitian operator trick)

Lapse and shift subroutines

Fixed lapse and shift steps:

1. amplitude encoding lapse function (grid + ancilla)
2. control operations on coin operators and ancilla
3. undo step 1

Note: we also looked into dynamical lapse and shift subroutines[5]

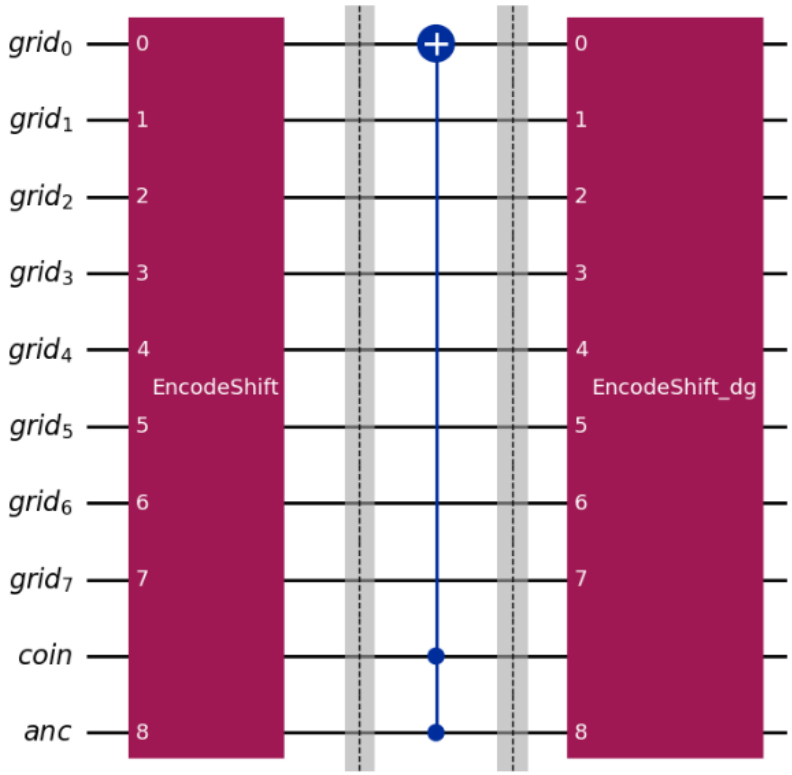

[5] Feel free to ask me about this

Boundaries

Absorbing boundaries $\leftrightarrow$ amplitude damping channel

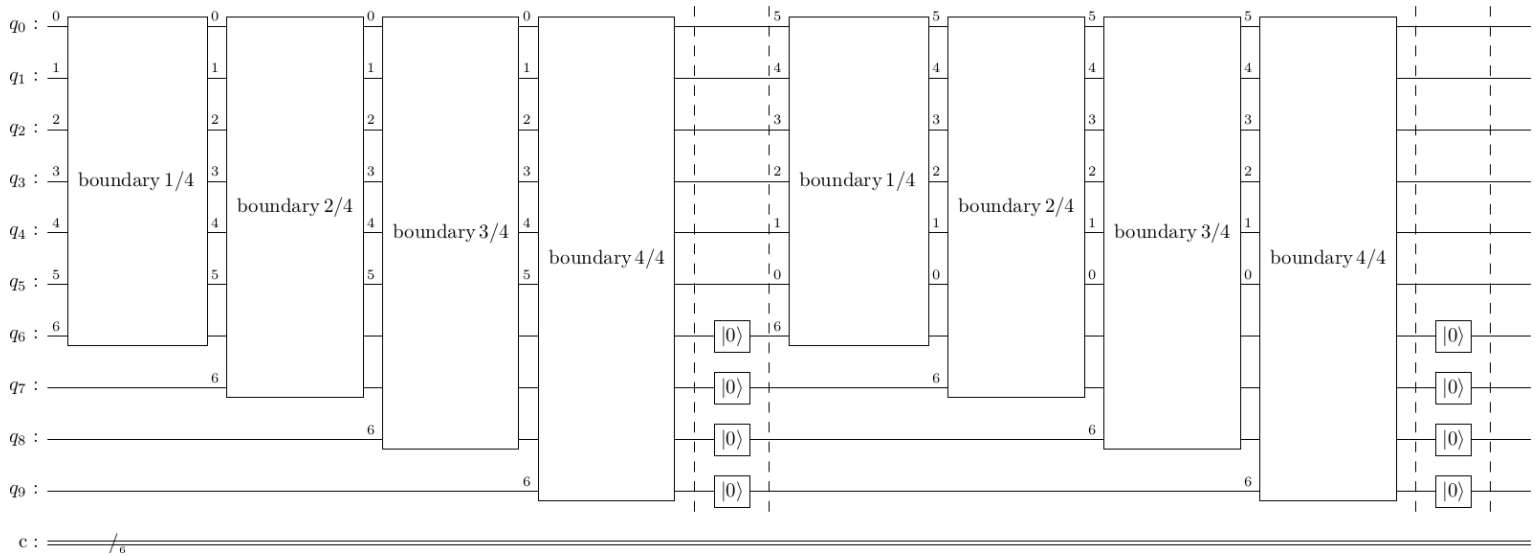

Figure: Absorbing boundaries

Testing the algorithm

Schwarzschild BH stationary solution

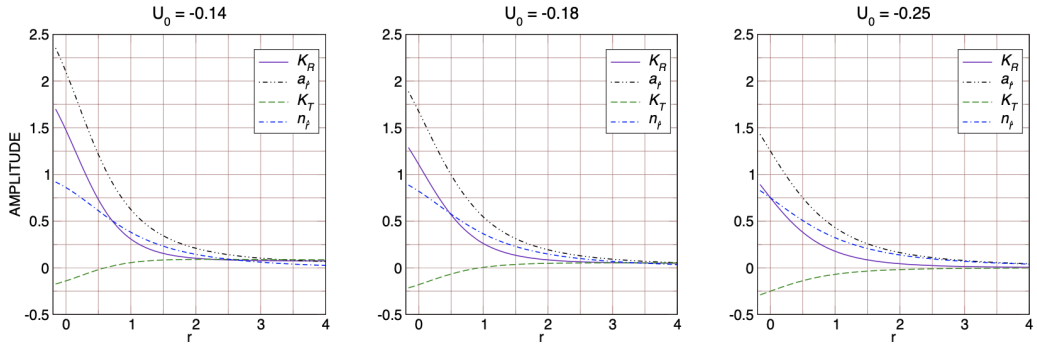

FIG. 1: Stationary Schwarzschild solution, Nester gauge. Shown is the region $-0.16 < r < 4.0$. The outer boundary is located at $r = 9.84$.

Figure: Stationary solution from [Buchman and Bardeen, 2005]

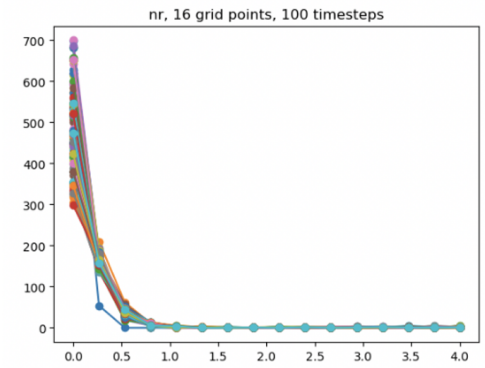

Figure: coordinate singularity close to horizon.

Schwarzschild BH stationary solution

- Poisson (shot) error
- leakage error

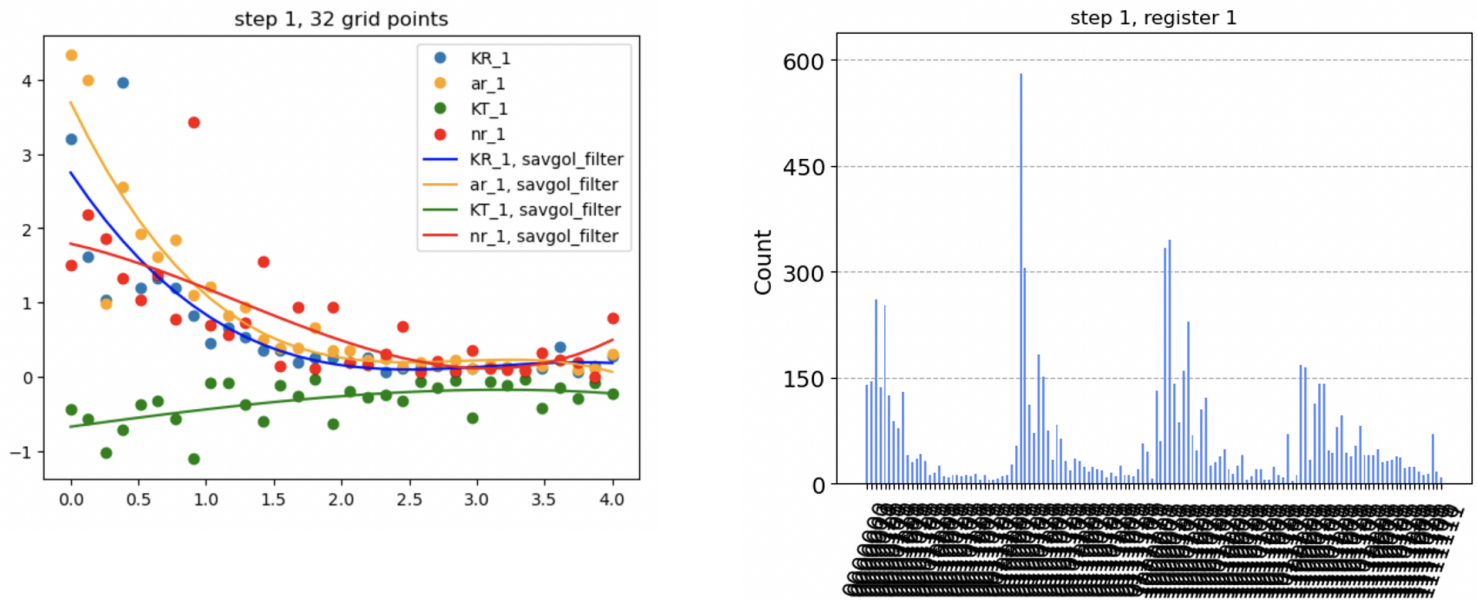

Figure: sources of error

Schwarzschild BH stationary solution

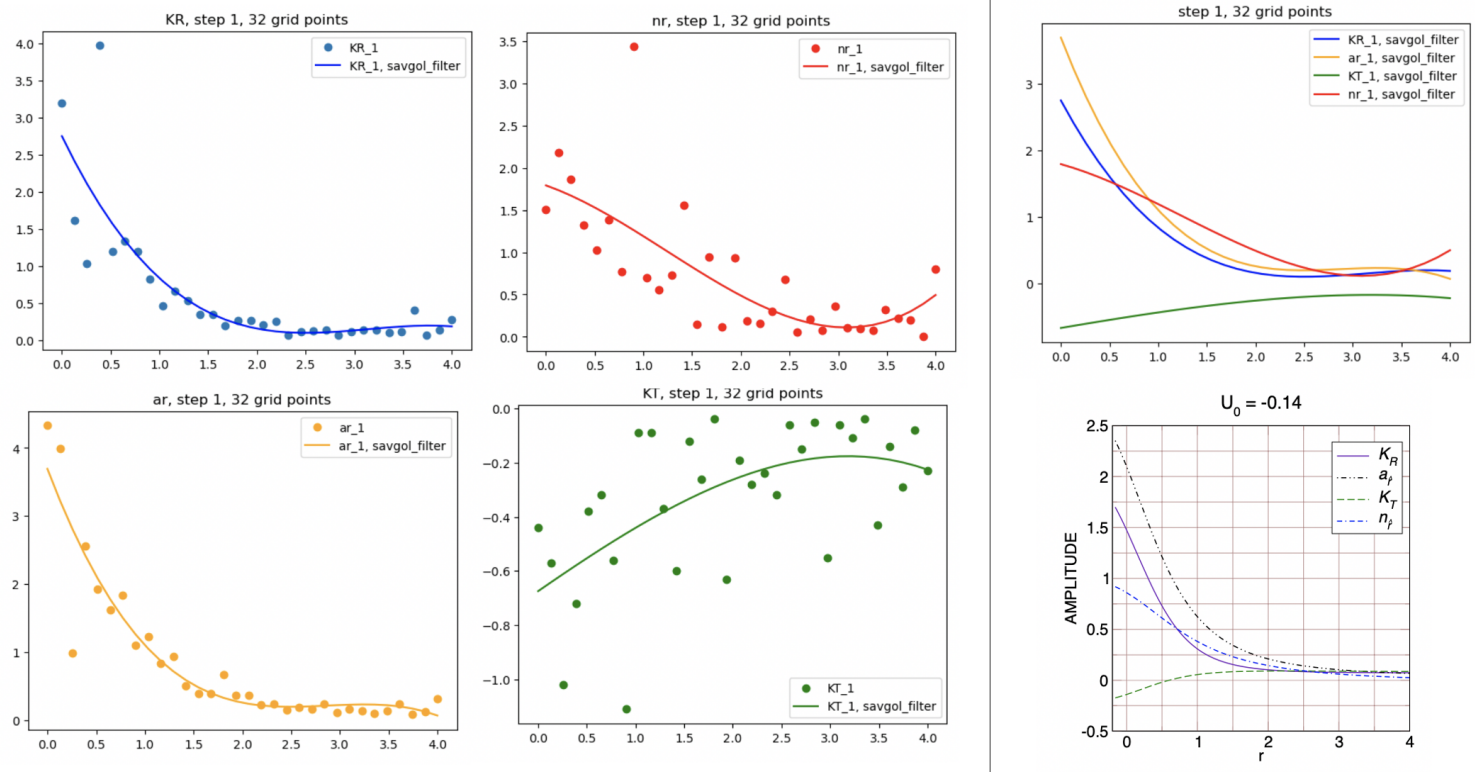

Figure: strategies to minimise error

Quasinormal modes

- As a means to test the quantum algorithm beyond the stationary Schwarzschild solution, we consider quasinormal modes, which are resonant frequencies of a perturbed black hole that obey the Zerilli/Regge-Wheeler functions [7, 8].

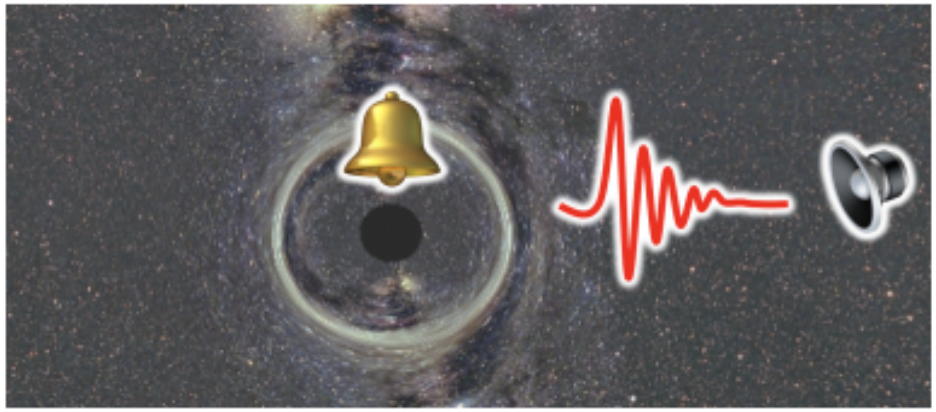

Fig. 5: Schematic representation of black hole quasinormal modes and their detection. The red wave corresponds to the Regge-Wheeler/Zerilli scalar [8], that depending on the spin of the perturbation, can be related to different observables (e.g. Ψ_4 for s spin-2 gravitational perturbation).

Quasinormal modes: classical code

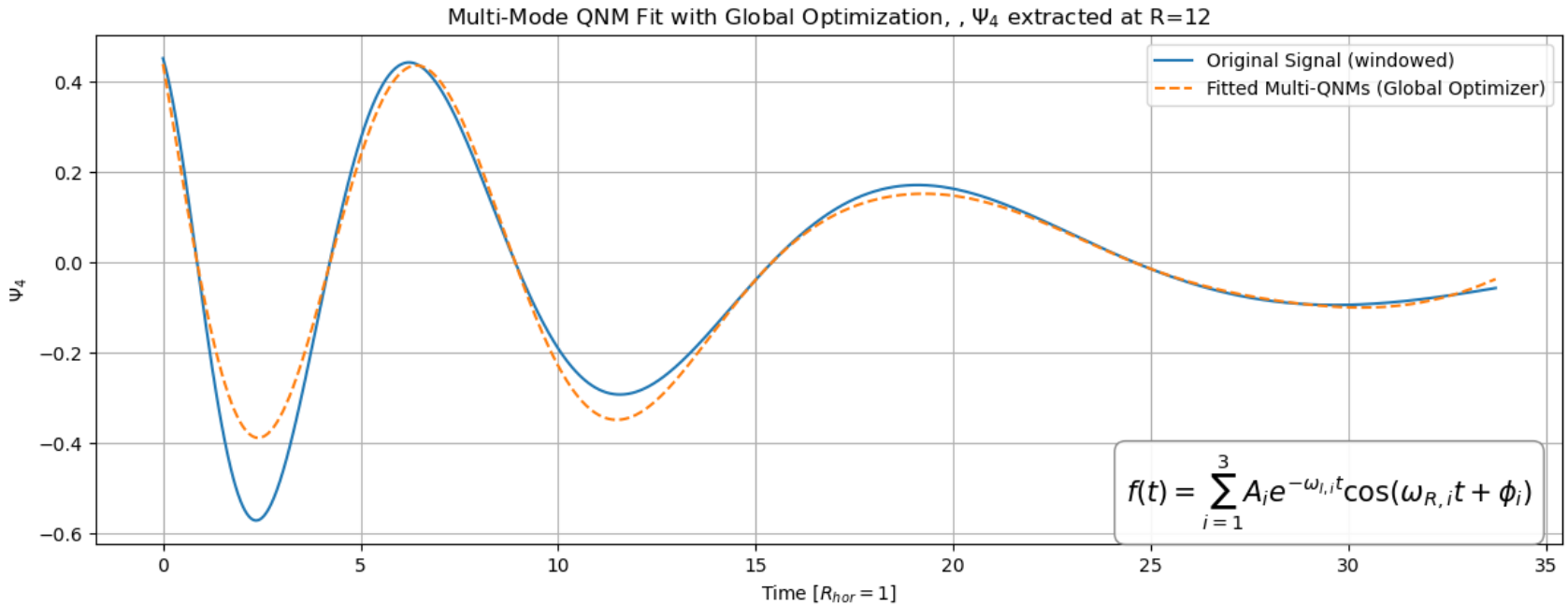

Extracted QNM Parameters (frequencies[MR^{-1}] multiplied by M and redhsifted):

```
Mode 1: A = 0.805 ± 0.010, ω_R = 0.371 ± 0.002, ω_I = 0.093 ± 0.002, ϕ = 0.720 ± 0.025
Mode 2: A = 0.239 ± 0.015, ω_R = 0.265 ± 0.000, ω_I = 0.030 ± 0.002, ϕ = 2.733 ± 0.012
Mode 3: A = 0.181 ± 0.004, ω_R = 0.173 ± 0.000, ω_I = 0.005 ± 0.001, ϕ = 5.010 ± 0.015
```

Quasinormal modes: Qiskit simulation

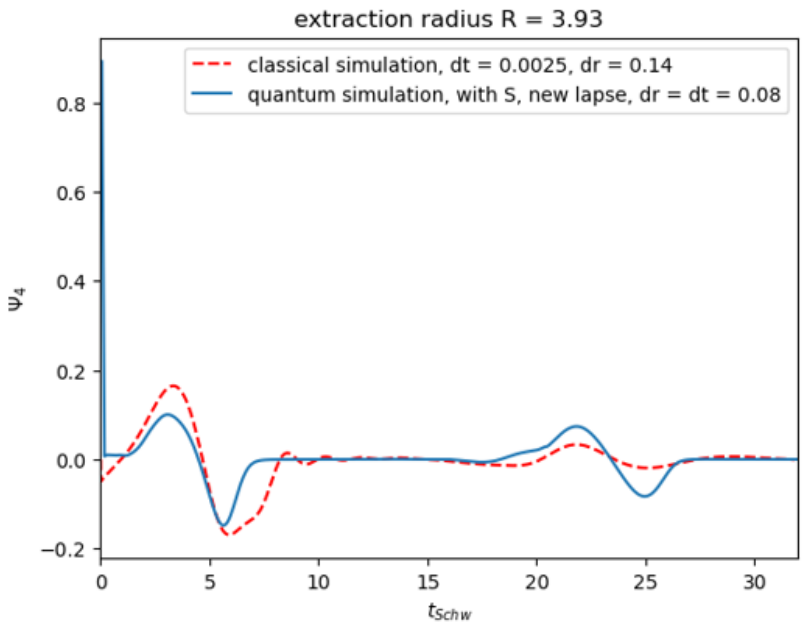

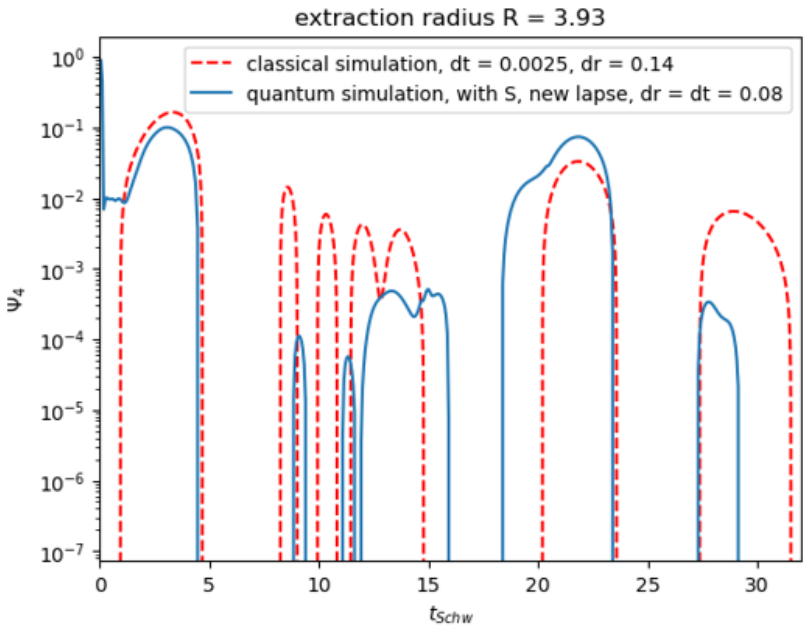

Quasinormal modes: IBM Quantum computers

Work in progress: figuring out noise, error mitigation techniques and future improvements

Conclusion and future work

- first quantum algorithm for NGR;
- first time WEBB formalism is used for QNMs;
- QNMs features (e.g. overtones) $\leftrightarrow$ form of S, entanglement and superpositions, fuzzy horizons, QG applications?
- extend to include energy-momentum tensor or different physical systems interesting for Cosmology.
- error and noise mitigation;

Comments/suggestions: clelia.altomonte@kcl.ac.uk

Backup slides

Tetrads and Ricci Rotation coefficients: Physical interpretation

Physical interpretation of Ricci Rotation coefficients:

- $a_a \equiv \Gamma_{a00}$ acceleration of the congruence relative to Fermi-Walker transport (FWT);
- $\omega_a \equiv \frac{1}{2}\varepsilon_{abc}\Gamma_{cb0}$ angular velocity of the spacelike triads relative to FWT;
- $N_{ab} \equiv \frac{1}{2}\varepsilon_{bcd}\Gamma_{cda}$ connection coefficients involving only spatial components of the tetrad. N_{11}, N_{22}, and N_{33} describe twists of the spatial triads along the $1, 2, 3$ direction. Combinations $N_{ab} + N_{ba}$ of the non-diagonal components represent gravitational wave degrees of freedom. It is convenient to represent the antisymmetric part of N_{ba} by its own symbol $n_a \equiv \frac{1}{2}\varepsilon_{abc}N_{bc}$.
- $K_{ab} \equiv \Gamma_{b0a}$. More generally, the symmetric part of K_{ba} is the rate of strain of the congruence, and its antisymmetric part, $\Omega_a \equiv \frac{1}{2}\varepsilon_{abc}K_{bc}$, the vorticity of the congruence. If $\Omega_a = 0$, the congruence is hypersurface orthogonal, and K_{ba} is the traditional extrinsic curvature of the orthogonal hypersurface.

Tetrads and Ricci Rotation coefficients

Fermi-Walker transport (FWT):

- defines reference frames s.t. all curvature is due to presence of mass/energy density, not of arbitrary spin or rotation of the frame.
- a generalization of covariant differentiation (for inertial frames, Fermi–Walker derivatives reduce to covariant derivatives).
- stipulate Fermi–Walker derivatives $\frac{D_F X}{ds} = 0$ should vanish, where, for vector field X along curve $\gamma(s)$ ($(-+++)$ signature):

$$\frac{D_F X}{ds} = \frac{DX}{ds} - \left(X, \frac{DV}{ds}\right) V + (X, V) \frac{DV}{ds} \tag{7}$$

with four-velocity V, covariant derivative D, and scalar product $(\cdot, \cdot)$.

Lattice-Boltzmann method $\leftrightarrow$ Quantum walk

1. Lattice-Boltzmann method:
   - Navier-Stokes equations of classical fluid-dynamics emerge from the Boltzmann equation in given limit (as function of mean-free-path and typical macroscopic scale).
   - fictive particles perform propagation and collision steps over a discrete lattice.

2. spin-boson d.o.f.s $\leftrightarrow$ Dirac Hamiltonian.

3. Quantum walk:
   - random walk aided by quantum superposition, unitary evolution, collapse.
   - Product state of internal spin and position, $|\Psi\rangle = |s\rangle \otimes |\psi\rangle$, where

$$|s\rangle \in \mathcal{H}_C = \left\{ a_\uparrow |\uparrow\rangle + a_\downarrow |\downarrow\rangle : a_{\uparrow/\downarrow} \in \mathbb{C} \right\} \tag{8}$$

$$|\psi\rangle \in \mathcal{H}_P = \left\{ \sum_{x\in\mathbb{Z}} \alpha_x |x\rangle : \sum_{x\in\mathbb{Z}} |\alpha_x|^2 < \infty \right\} \tag{9}$$

WEBB hyperbolic tetrad formalism

- connection formulation.
- Tetrad orthonormal basis vectors define local Lorentz frames $\boldsymbol{e}_\alpha (\alpha = 0, 1, 2, 3)$.
- spacetime metric is Minkowski everywhere: $g_{\alpha\beta} = \boldsymbol{e}_\alpha \cdot \boldsymbol{e}_\beta = \eta_{\alpha\beta}$, with dual basis $e^\alpha : \left\langle \boldsymbol{e}^\alpha, \boldsymbol{e}_\beta \right\rangle = \delta^\alpha_\beta; \boldsymbol{e}^\alpha \cdot \boldsymbol{e}^\beta = \eta^{\alpha\beta}$.
- 24 distinct connection coefficients (also known as Ricci rotation coefficients) that transform as scalar fields under coordinate transformations and are anti-symmetric in the final two indices:

$$\Gamma_{\alpha\beta\gamma} = \boldsymbol{e}_\alpha \cdot \nabla_\gamma \boldsymbol{e}_\beta = -\Gamma_{\beta\alpha\gamma}$$

with ∇ being the covariant derivative operator with respect to a tetrad component (notice it is equivalent to a simple derivative, due to the trivial metric);

WEBB evolution equations

Evolution equation for the connection coefficients:

$$D_0\mathbf{q} + M^a D_a\mathbf{q} = \mathbf{S} \tag{10}$$

where:

- $\mathbf{q}$ is a vector of the 24 possible connection coefficients, arranged in four variables $N_{ab}, K_{ab}, a_a, \omega_a$;
- M^a is a sparse, unitary matrix;
- D_0 the derivative with respect to the tetrad congruence;
- D_a is the spatial derivative with respect to the tetrad spatial components.

WEBB is First Order Hyperbolic Symmetrizable (FOSH)

3+1 split, lapse and shift

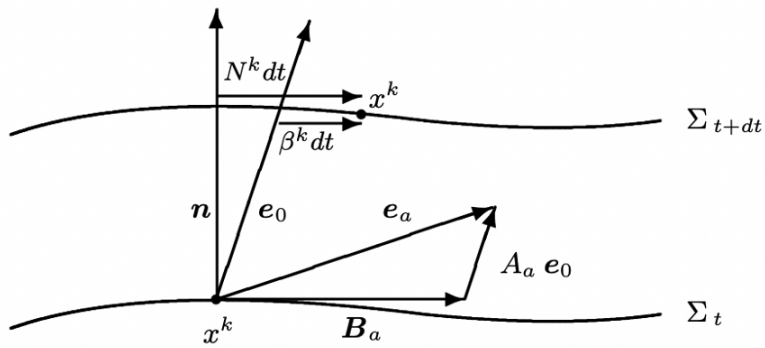

Figure: 3+1 split

- tetrad lapse function $\alpha =$ rate of change of proper time with respect to coordinate time along the tetrad congruence;
- tetrad shift vector $\beta^k =$ rate of displacement of the spatial coordinates relative to the tetrad congruence worldlines per unit coordinate time;

Given a choice of coordinates $\boldsymbol{e}_\alpha = \lambda^\mu_\alpha \boldsymbol{e}_\mu$:

$$\boldsymbol{e}_a = A_a \boldsymbol{e}_0 + \boldsymbol{B}_a \tag{11}$$

$$D_0 = \frac{1}{\alpha}\left(\frac{\partial}{\partial t} - \beta^k \frac{\partial}{\partial x^k}\right), D_a = A_a D_0 + B^k_a \frac{\partial}{\partial x^k} \tag{12}$$

Coordinates and Gauge - I

- Simulation $\rightarrow$ Schwarzschild coordinates:

$$dt_S = \frac{\alpha}{1 - Rn_{\hat{r}}} dt_s \tag{13}$$

Notice in ref. []: $M = 1/2, R = 2M = 1$, but plots use the convention that $R_{horizon} = 0$.

- Schwarzschild $\rightarrow$ Eddington-Finkelstein coordinates:

$$r^* = r + 2GM \ln \left| \frac{r}{2GM} - 1 \right| . \tag{14}$$

- outgoing Eddington–Finkelstein coordinates

$$u = t - r^* \tag{15}$$

$$ds^2 = - \left(1 - \frac{2GM}{r} \right) du^2 - 2dudr + r^2 d\Omega^2 \tag{16}$$

Coordinates and Gauge - II

- Nester Gauge: "The special or thonormal frames are just those which make the metric conformally flat and the special function is the conformal factor. " []
- sanity check for Ψ_4:

$$K_{ab} = S_{ab} - \Omega_c \varepsilon_{acb} \tag{17}$$

where S_{ab} is the symmetric rate-of-strain 3-tensor of the observer fluid, and Ω_c is its axial vector of vorticity.

Cauchy problem, well-posedness [6]

Given suitable initial data on a (non-characteristic) Cauchy surface Σ_0 that satisfies the constraints, the initial value problem is well-posed if

1. there exists a unique solution of the equations of motion,
2. the solution depends continuously on the initial data (in a suitable norm), e.g.

$$\|\Phi\|_{H^S}(t) \leq C(t)\|\Phi\|_{H^S}(0) \tag{18}$$

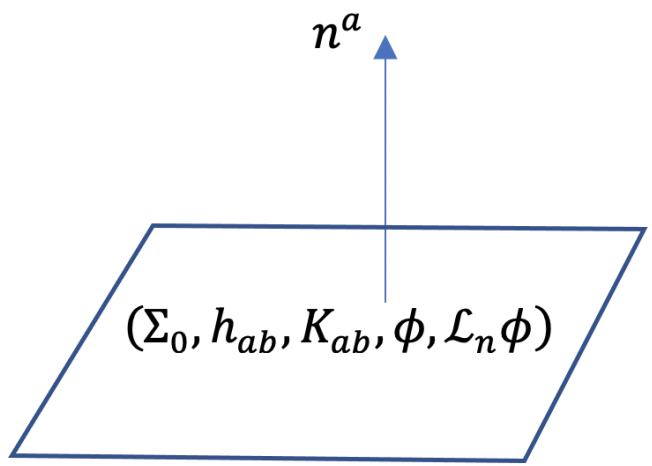

Figure: Cauchy problem (adapted from A.K., London Gravity Meeting, 28/2/24)

[6] synthesis borrowed from A.K.'s presentation, London Gravity Meeting, 28/2/24

Hyperbolicity[7]

Consider a first order linear system of pdes with constant coefficients

$$\partial_i u = M^i \partial_i u + Nu \tag{19}$$

Then one can find the solution by taking the Fourier transform

$$u(t,x) \propto \int d^d\xi e^{i\xi_k x^k} e^{\left(iM^k\xi_k + N\right)t} \bar{u}(0,\xi) \tag{20}$$

For the integral to converge and the IVP be well-posed, we need

$$\left\| e^{iM^k\xi^t} \right\| \leq f(t) \quad \text{for any } \xi \in \mathbb{R}^d \tag{21}$$

It can be shown that this implies $M(\xi) \equiv M^k\xi_t$ admits a symmetrizer $K(\xi)$: a positive definite and bounded Hermitian matrix satisfying

$$K(\xi)M(\xi) = M^\dagger(\xi)K(\xi) \tag{22}$$

We say that a pde satisfying this condition is strongly hyperbolic. The IVP for strongly hyperbolic pdes is locally well-posed.

[7] synthesis borrowed from A.K.'s presentation, London Gravity Meeting, 28/2/24

Hyperbolicity for nonlinear pdes[8]

For nonlinear pdes consider

$$\partial_t u = F\left(t, x, u, \partial_t u\right) \tag{23}$$

$$M(t, x, u, \partial, u; \xi) \equiv \frac{\partial F}{\partial\left(\partial_k u\right)} \xi_k \tag{24}$$

System is strongly hyperbolic if M admits a positive definite symmetrizer $K(t, x, u, \partial, u; \xi)$ that depends smoothly on its arguments and is bounded.

The IVP for strongly hyperbolic nonlinear pdes is locally well-posed.

[8] synthesis borrowed from A.K.'s presentation, London Gravity Meeting, 28/2/24

Collision

Write the Jacobian matrix

$$\mathbf{J_f}(K_R, a_r, K_T, n_r) = \begin{bmatrix} \frac{\partial f_1}{\partial K_R} & \frac{\partial f_1}{\partial a_r} & \frac{\partial f_1}{\partial K_T} & \frac{\partial f_1}{\partial n_r} \\ \frac{\partial f_2}{\partial K_R} & \frac{\partial f_2}{\partial a_r} & \frac{\partial f_2}{\partial K_T} & \frac{\partial f_2}{\partial n_r} \\ \frac{\partial f_3}{\partial K_R} & \frac{\partial f_3}{\partial a_r} & \frac{\partial f_3}{\partial K_T} & \frac{\partial f_3}{\partial n_r} \\ \frac{\partial f_4}{\partial K_R} & \frac{\partial f_4}{\partial a_r} & \frac{\partial f_4}{\partial K_T} & \frac{\partial f_4}{\partial n_r} \end{bmatrix} =$$

$$= \begin{bmatrix} -2K_R & 2a_r & 2K_T & -2n_r \\ K_T & -n_r & K_R - K_T & -2n_r \\ n_r & -K_T & a_r - 2n_r & K_R - 2K_T \\ 0 & 0 & 0 & 0 \end{bmatrix} + \begin{bmatrix} 0 & 0 & 0 & 2/R \\ 0 & 0 & 0 & 1/R \\ -1/R & 0 & 1/R & 0 \\ 2/R & 0 & -2/R & 0 \end{bmatrix} \quad (25)$$

Consider the parts of each of the transition matrix elements $x|y\rangle\langle z|$ as indicating:

- x the component present in a given matrix element;
- $|y\rangle \rightarrow$ which partial derivative has been applied;
- $\langle z| \rightarrow$ the row where the matrix element is located;

Schwarzschild ringdown Quasinormal modes

Decomposition into spherical harmonics for each $h_{\mu\nu}$ of the form

$$\chi(t, r, \theta, \phi) = \sum_{\ell m} \frac{\chi_{\ell m}(r, t)}{r} Y_{\ell m}(\theta, \phi) \tag{26}$$

The Regge-Wheeler function (axial or odd-parity d.o.f.s):

$$\Box^{\{1\}} \Phi_\ell^m - V_{\mathrm{RW}}{}^{\{1\}} \Phi_\ell^m = 0 \tag{27}$$

with $V_{\mathrm{RW}} \equiv \frac{\ell(\ell+1)}{r^2} - \frac{6M}{r^3}$

Zerilli (polar or even d.o.f.s):

$$\Box^{\{1\}} \Psi_\ell^m - V_{\mathrm{Z}}{}^{\{1\}} \Psi_\ell^m = 0 \tag{28}$$

with $V_{\mathrm{Z}} \equiv \frac{\ell(\ell+1)}{r^2} - \frac{6M}{r^3} \frac{r^2\lambda(\lambda+2)+3M(r-M)}{(r\lambda+3M)^2}$, $\lambda \equiv \frac{1}{2}(\ell-1)(\ell+2)$

- In our case: perturb K_T and n_r: spherical $\rightarrow$ axial symmetry $\rightarrow$ gravitational d.o.f.s allowed.

Quasinormal modes

Newman-Penrose (NP) formalism $\rightarrow$ Weyl scalar Ψ_4: outgoing gravitational d.o.f.s (TT gauge)

$$\Psi_4 = \frac{1}{2}\left(\ddot{h}_{\hat{\theta}\hat{\theta}} - \ddot{h}_{\hat{\phi}\hat{\phi}}\right) + i\ddot{h}_{\hat{\theta}\hat{\phi}} = -\ddot{h}_{+} + i\ddot{h}_{\times} \tag{29}$$

where

$$\frac{1}{4}\left(\ddot{h}_{\theta\theta} - \ddot{h}_{\phi\phi}\right) = -R_{\theta t\theta t} \tag{30}$$

$$\frac{1}{2}\ddot{h}_{\theta\phi} = -R_{r\theta t\phi} \tag{31}$$

using

$$R_{\alpha\beta\gamma\delta} = D_\gamma \Gamma_{\alpha\beta\delta} - D_\delta \Gamma_{\alpha\beta\gamma} + \Gamma_{\alpha\varepsilon\gamma}\Gamma^{\epsilon}_{\beta\delta} - \Gamma_{\alpha\varepsilon\delta}\Gamma^{\varepsilon}_{\beta\gamma} + \Gamma_{\alpha\beta\varepsilon}\left(\Gamma^{\varepsilon}_{\gamma\delta} - \Gamma^{\varepsilon}_{\delta\gamma}\right) \tag{32}$$

and finally, since $\Psi_4 := C_{abcd} n^a \bar{m}^b n^c \bar{m}^d$, project onto the null tetrad defined as

$$\begin{aligned} n^\mu &= \frac{1}{\sqrt{2}}(\hat{t} - \hat{r}) \\ \bar{m}^\mu &= \frac{1}{\sqrt{2}}(\hat{\theta} - i\hat{\phi}) \end{aligned} \tag{33}$$

References I

(N.d.[b]). URL: https://www.arturekert.org/iqis.

Buchman, L. T. and J. M. Bardeen (2005). "Schwarzschild tests of the Wahlquist-estabrook-buchman-bardeen tetrad formulation for numerical relativity". In: *Physical Review D* 72.12. DOI: 10.1103/physrevd.72.124014.

Feynman, Richard P (June 1982). "Simulating physics with computers". en. In: *Int. J. Theor. Phys.* 21.6-7, pp. 467–488.

Fillion-Gourdeau, François, Steve MacLean, and Raymond Laflamme (2017). "Algorithm for the solution of the Dirac equation on digital quantum computers". In: *Physical Review A* 95.4. DOI: 10.1103/physreva.95.042343.

Kim, Youngseok et al. (June 2023). "Evidence for the utility of quantum computing before fault tolerance". en. In: *Nature* 618.7965, pp. 500–505.

Nielsen, Michael A. and Isaac L. Chuang (2012). In: *Quantum Computation and Quantum Information*. DOI: 10.1017/cbo9780511976667.

Succi, Sauro, François Fillion-Gourdeau, and Silvia Palpacelli (2015). "Quantum lattice Boltzmann is a quantum walk". In: *EPJ Quantum Technology* 2.1. DOI: 10.1140/epjqt/s40507-015-0025-1.